

High spin states in ^{175}Ta : An acute example of delayed crossing frequency

Shu-Xian Wen, Hua Zheng, Sheng-Gang Li, Guang-Sheng Li, Guan-Jun Yuan, Peng-Fei Hua, Pei-Kun Weng,
Lan-Kuan Zhang, Pan-Shui Yu, and Chun-Xiang Yang
China Institute of Atomic Energy, P.O. Box 275, Beijing 102413, People's Republic of China

Hui-Bin Sun,* Ya-Bo Liu, and Yun-Zuo Liu
Department of Physics, Jilin University, Changchun, Jilin 130023, People's Republic of China

Yang Sun† and Da Hsuan Feng
Department of Physics and Atmospheric Science, Drexel University, Philadelphia, Pennsylvania 19104
(Received 11 March 1996)

High spin states in ^{175}Ta are populated by the $^{160}\text{Gd} (^{19}\text{F}, 4n) ^{175}\text{Ta}$ reaction. This experiment, carried out at the HI-13 tandem accelerator at the China Institute of Atomic Energy which measured the γ - γ coincidences, gives rise to a new level scheme. Two important new features are embedded in this scheme. First, the seven decay sequences built on $\frac{1}{2}^- [541]$, $\frac{7}{2}^- [404]$, $\frac{5}{2}^- [402]$, and $\frac{9}{2}^- [514]$ proton Nilsson configurations are significantly extended to higher spins. For example, for the $\frac{1}{2}^- [541]$ band, the levels have extended from $\frac{33}{2}^-$ to $\frac{61}{2}^-$ and, for the $\frac{7}{2}^- [404]$ band, from $\frac{21}{2}^-$ to $\frac{41}{2}^-$. Second, compared to the neighboring even-even nuclides, the neutron AB crossing frequency built on the $h_{7/2}^+$ proton Nilsson state $\frac{1}{2}^- [541]$ is significantly larger, which according to the conventional cranking shell model (CSM) is an anomaly. In this paper, this large crossing frequency is also discussed within the framework of the projected shell model. It is shown that this anomaly found in CSM can be satisfactorily explained, thus suggesting an alternative understanding. [S0556-2813(96)00909-0]

PACS number(s): 21.10.Re, 23.20.Lv, 21.60.Cs, 27.70.+q

I. INTRODUCTION

An interesting phenomenon of the rare-earth high spin spectroscopy is the observation of a significantly delayed proton $\frac{1}{2}^- [541]$ band crossing frequency: The crossing frequency of this band in certain odd- Z nuclei is much higher than their even-even neighbors. This phenomenon was noticed previously in conjunction with the study of back-bending effects [1–4]. With the coming on line of large detector arrays and with new theoretical models, there is renewed interest in this phenomenon (see, e.g. [5–7], for an empirical systematic study of the crossing delay and [8–11] for theoretical discussions).

Recently, a number of studies on odd Ta isotopes were performed [12–16] to understand this phenomenon. The results showed that only the neutron AB crossing for the $\frac{1}{2}^- [541]$ band in the odd-Ta isotopes manifests such a delay. It is known that the first band crossing for rare earths is due to the alignment of the $i_{13/2}$ quasineutron pair. Since the Fermi levels for protons and neutrons in this mass region occur in different major shells, one would expect the band crossings to exhibit a weak dependence on the odd proton in the odd-even nucleus and hence no delay in the crossing frequency. While this is true for most proton bands, it is not true for the $\frac{1}{2}^- [541]$ band. In fact, the delay is observed systematically not only in the Ta isotopes, but also in other odd- Z rare earths, e.g., ^{157}Ho [17], ^{163}Tm [6], ^{165}Lu [18], ^{167}Lu [5], and ^{171}Re [19].

The choice of using ^{175}Ta for the present purpose is motivated as follows. Yang *et al.* have previously speculated [20] that this delay may be caused by the core being polarized by the odd $\frac{1}{2}^- [541]$ proton (see also Refs. [4,5]). If this were true, then the very large orbital quadrupole moment ($q_2 = 3n_z - N = 7$) and the dominant particle nature of the $\frac{1}{2}^- [541]$ quasiproton band should then “drive” the core to be even more prolate. Thus, the “smoking gun” of this speculation hinges on how close the $\frac{1}{2}^- [541]$ proton Nilsson orbit is to the Fermi surface, because the closer it is, the smaller the delay. There are two ways to bring the $\frac{1}{2}^- [541]$ Nilsson orbit closer to the Fermi level: by increasing Z or increasing the quadrupole deformation ϵ_2 . Hence, the nucleus ^{175}Ta is the best testing ground for the study of the delay in the crossing frequency because, according to Lund systematics [21], it has the largest quadrupole deformation ϵ_2 among the Ta isotopes and therefore should have only a small, if any, delay.

We note that although high spin states for the bands $\frac{7}{2}^- [404]$, $\frac{5}{2}^- [402]$, $\frac{9}{2}^- [514]$, and $\frac{1}{2}^- [541]$ of ^{175}Ta were previously measured by Foin *et al.* [22], they were not high enough for the present study. For example, the highest spin state of the $\frac{1}{2}^- [541]$ band measured by Foin *et al.* was below the first band crossing. This paper will present the results of this extension. Some preliminary results were previously reported [23].

The content of the present paper is organized as follows: In Sec. II, the experimental procedure and the new level scheme are given. Consequences of various model predictions regarding the delayed crossing frequency for the $\frac{1}{2}^- [541]$ band are discussed in Secs. III and IV. In Sec. III, we conclude from the various analyses using the conventional cranked shell model (CSM) that the CSM cannot quantitatively reproduce the observed delay. In Sec. IV, the projected

*Present address: Department of Physics, Florida State University, Tallahassee, Florida 32306.

†Present address: Joint Institute for Heavy Ion Research, Oak Ridge National Laboratory, Oak Ridge, Tennessee 37831.

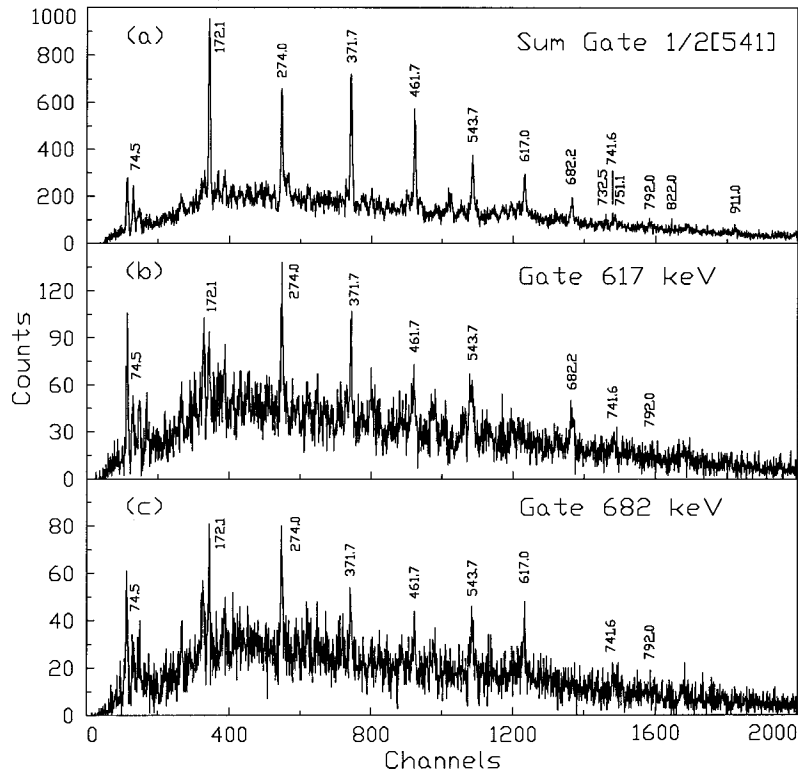


FIG. 2. Spectra gated on (a) $\frac{1}{2} [541]$ sum gate, (b) 617 keV, and (c) 682 keV.

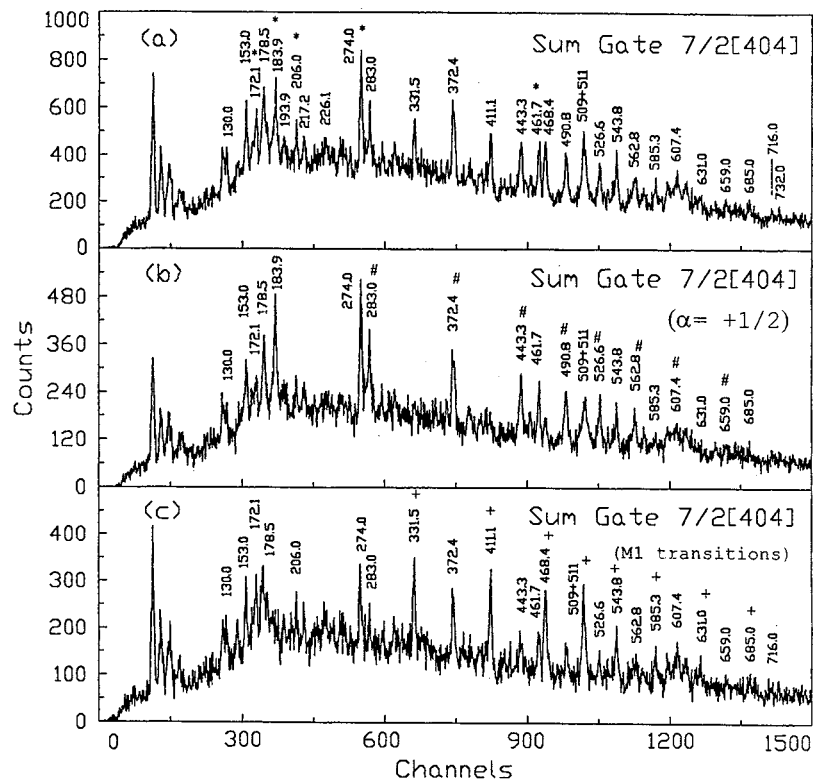


FIG. 3. Sum-gate spectra of (a) $\frac{7}{2} [404]$ band (the peaks marked with an asterisk are contaminated from other bands), (b) $\alpha = +1/2$ $E2$ transitions (marked with #), and (c) $M1$ transitions ($\alpha = -1/2$ $E2$ transitions marked with +).

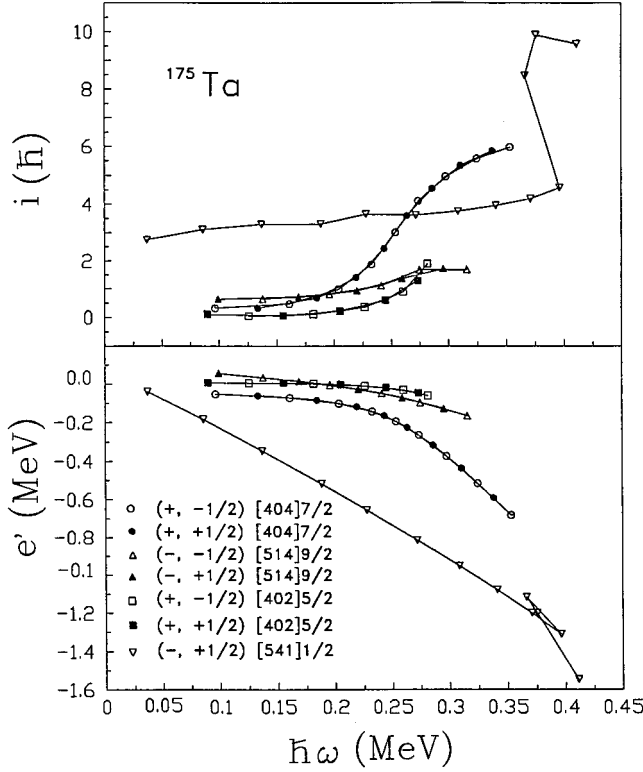


FIG. 4. Experiment Routhians and alignments of ^{175}Ta , with Harris parameter $\mathcal{H}_0 = 30 \text{ MeV}^{-1} \hbar^2$ and $\mathcal{H}_1 = 70 \text{ MeV}^{-3} \hbar^4$.

D. Experimental data in the rotational frame

In order to study the effect of rotation on the single-particle motion, we shall transform the experimentally measured excitation energies and spins into the intrinsic rotating frame [24,25]. The experimental quasiparticle spin alignments and the Routhians plotted as functions of the rotational frequency $\hbar\omega$ for ^{175}Ta are displayed in Fig. 4. The Harris parameters of the rotational reference configuration are $\mathcal{H}_0 = 30 \text{ MeV}^{-1} \hbar^2$ and $\mathcal{H}_1 = 70 \text{ MeV}^{-3} \hbar^4$. We noticed that the neutron AB band crossing frequency for the band built on the $\frac{1}{2}$ [541] proton configuration is about $0.375 \text{ MeV}/\hbar$, which is the highest one so far observed in this mass region. The delay frequencies observed in ^{157}Ho [17] and ^{163}Tm [6] are comparable in magnitude to this one.

E. $B(M1)/B(E2)$ values

One can deduce the empirical $B(M1)/B(E2)$ ratios from the observed γ -ray energies E_γ and branching ratios λ as follows:

$$\frac{B(M1; I \rightarrow I-1)}{B(E2; I \rightarrow I-2)} = 0.697 \frac{E_\gamma^5(I \rightarrow I-2)}{E_\gamma^3(I \rightarrow I-1) \lambda (1 + \delta^2)}. \quad (1)$$

For the cases here, the factor δ^2 is sufficiently small and is neglected.

Likewise, by using the semiclassical formula [26] which assumes a small γ deformed rotational model for the $B(E2)$'s [27], one can compute the $B(M1)/B(E2)$ ratios:

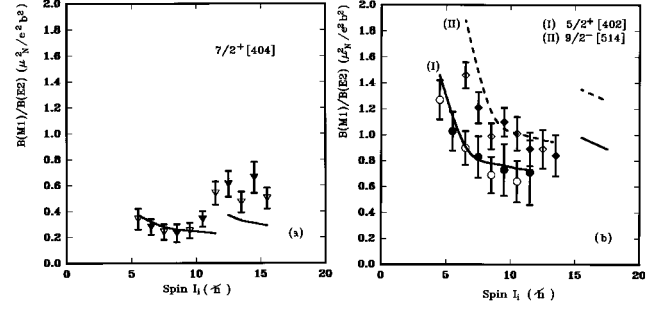


FIG. 5. Experimental $B(M1)/B(E2)$ values as a function of spin for the bands in ^{175}Ta . The curves are theoretical predictions (see text).

$$\frac{B(M1; I \rightarrow I-1)}{B(E2; I \rightarrow I-2)}$$

$$= \frac{12}{5Q_0^2[\cos^2(30^\circ)]} \left[1 - \frac{K^2}{\left(1 - \frac{1}{2}\right)^2} \right]^{-2} K^2 \left((g_p - g_R) \right. \\ \left. \times \left[\left[1 - \left(\frac{K}{I}\right)^2 \right]^{1/2} - \frac{i_p \pm \Delta e'}{I} \pm \frac{\Delta e'}{\hbar\omega} \right] - (g_n - g_R) \frac{i_n}{I} \right)^2, \quad (2)$$

where g_R is the g factor of the collective rotation, g_p (g_n) the intrinsic g factor of the quasiproton (quasineutron), and i_p and i_n aligned angular momentum for the proton and neutron, respectively. The term $\Delta e'/\hbar\omega$ is the relative experimental signature splitting and $K=K(\omega)$ the frequency-dependent effective K value in accordance with the prescriptions given by Ref. [26]. Q_0 is the quadrupole moment for the relevant configuration. In the present calculation, g_R is assumed to be 0.4 (0.3) below (above) the crossing point. This variation of the g_R accounts for the increased neutron contribution. Also, the g_p values were obtained for each band from the Nilsson calculations: $g_p=1.36$ for $\frac{9}{2}$ [514], $g_p=1.50$ for $\frac{5}{2}$ [402], and $g_p=0.72$ for $\frac{7}{2}$ [404]. The g_n value, on the other hand, was assumed to be -0.2 . For the quadrupole moment (Q_0), we have used 6.9 ($e b$) for $\frac{5}{2}$ [402] and 7.3 ($e b$) for both $\frac{9}{2}$ [514] and $\frac{7}{2}$ [404], which assumes that Q_0 is proportional to the ε_2 deformation [28]. Finally, the alignments i_p and i_n were taken directly from the experimental results. The present calculations were carried out without any signature splitting and the results are displayed in Fig. 5. Obviously, below the neutron crossing point, there is reasonable agreement for all three bands between the theory and the data. However, beyond the neutron crossing for band $\frac{7}{2}$ [404], the theory fails to reproduce the data. One should note that the neglect of δ in determining the experimental ratios requires generally a smaller Q_0 [13].

III. ANALYSIS WITH THE CRANKED SHELL MODEL

A. Neutron AB band crossing frequencies for the $\frac{1}{2}$ [541] proton configuration

The experimental ω_c extracted from the Routhian plot is approximately $0.375 \text{ MeV}/\hbar$. This is significantly larger by about 80 keV than those of the yrast sequences of its even-

TABLE II. Comparison of the band crossing frequencies of ^{174}Hf , ^{175}Ta , and ^{176}W .

| Nucleus | Rotational band | $\hbar\omega_c$ (MeV) |
|-------------------|---------------------|-----------------------|
| ^{174}Hf | Yrast | 0.292 |
| ^{175}Ta | $\frac{1}{2}$ [541] | 0.375 |
| ^{176}W | Yrast | 0.291 |

even neighbors ^{174}Hf [29] and ^{176}W [30] (see Table II). In fact, this delay in crossing frequency is so far the largest observed in the $\frac{1}{2}$ [541] band in odd-Ta isotopes (see Table III) or any other odd- Z nuclei of this region. It is interesting to note that the shift $\Delta\hbar\omega_c = \hbar\omega_c(o-e) - \hbar\omega_c(e-e)$ in the odd-Ta isotopes forms a V shape with increasing neutron number with a minimum at $N=98$. As mentioned in Sec. I, this shift may be due to the so-called ε_2 deformation driving effect of the $\frac{1}{2}$ [541] proton with a larger prolate orbital momentum. It is worth noting that in the same nucleus one obtains also a lower crossing frequency by about 40 keV (0.25 MeV/ \hbar) than its immediate even-even neighbors for the $\frac{7}{2}$ [404] band. This is the lowest crossing frequency in the [404] band for the odd- Z Ta nuclei. Thus this means that the oblate orbital quadrupole moment here ($q_2 = 3n_z - N = -4$) should reduce the prolateness of the core. One may conclude from this discussion that the shift in the crossing frequency is partially due to some shape driving effect and should be configuration dependent.

B. CSM calculation for $\frac{1}{2}$ [541] proton configuration

In this section, we shall use the CSM to analyze the data. Three versions of the CSM calculations are performed. In the first two calculations, the Nilsson parameters from Ref. [31] are used.

The parameters for the first version are $\varepsilon_2 = 0.250$, $\varepsilon_4 = 0.032$ (taken from Möller and Nix [21]), and a pairing gap of $\Delta_n = 0.730$ MeV which is extracted from the odd-even mass difference formula

$$\Delta_n = \frac{1}{4}[B(Z, N-2) - 3B(Z, N-1) + 3B(Z, N) - B(Z, N+1)]. \quad (3)$$

The result of this calculation gives an AB band crossing frequency of 0.27 MeV/ \hbar , which is not only lower than the observed value for ^{175}Ta , but is also lower than its adjacent even-even nuclei ^{174}Hf ($\hbar\omega_c \sim 0.291$ MeV) and ^{176}W ($\hbar\omega_c \sim 0.293$ MeV).

TABLE III. Shift in crossing frequency for $\frac{1}{2}$ [541] band in Ta isotopes.

| Nucleus | $\hbar\omega_c$ (MeV) | Nucleus | $\hbar\omega_c$ (MeV) | Nucleus | $\hbar\omega_c$ (MeV) | $\Delta\hbar\omega_c$ (keV) |
|-------------------|-----------------------|-------------------|-----------------------|------------------|-----------------------|-----------------------------|
| ^{167}Ta | 0.295 | ^{166}Hf | 0.255 | ^{168}W | 0.245 | 45 |
| ^{169}Ta | 0.305 | ^{168}Hf | 0.260 | ^{170}W | 0.270 | 40 |
| ^{171}Ta | 0.290 | ^{170}Hf | 0.275 | ^{172}W | 0.275 | 15 |
| ^{173}Ta | 0.360 | ^{172}Hf | 0.290 | ^{174}W | 0.300 | 65 |
| ^{175}Ta | 0.375 | ^{174}Hf | 0.291 | ^{176}W | 0.292 | 83 |

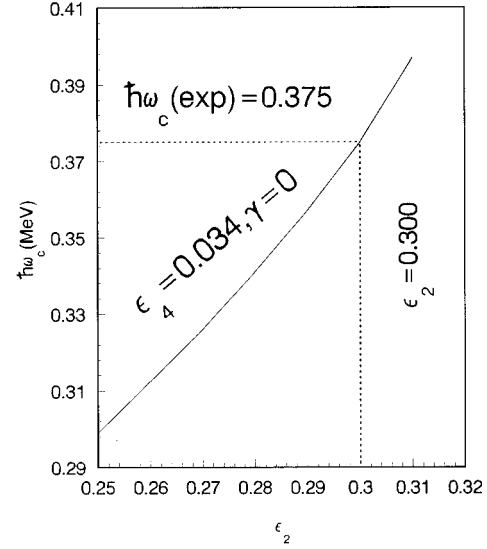


FIG. 6. Crossing frequency of the $\frac{1}{2}$ [541] band in ^{175}Ta vs the quadrupole deformation parameter ε_2 .

One possible reason why this calculation fails is because the pairing gap Δ_n is too small. To improve the agreement with the data, a second calculation utilizing an average pairing gap of 0.916 MeV is used. This gap is obtained by fitting the band crossing frequencies of the yrast sequence of its even-even neighbors ^{174}Hf ($\Delta_n = 0.843$ MeV) and ^{174}Hf ($\Delta_n = 0.990$ MeV). Unfortunately, this calculation also predicts too low a crossing frequency of 0.293 MeV/ \hbar , which is roughly 80 keV below the experimental value. In Fig. 6, we plot the change of the crossing frequency ω_c as a function of ε_2 with $\varepsilon_4 = 0.034$, $\gamma = 0$, and $\Delta_n = 0.916$ MeV. It shows that in order to reproduce the observed crossing frequency, the quadrupole deformation ε_2 should be around 0.30, a value which is neither consistent with the conventionally used deformation parameter given by Möller and Nix [21] nor the configuration-dependent deformation parameters of Nazarewicz, Riley, and Garrett [28]. The configuration-dependent deformation has been shown from a recent lifetime measurement [17]. However, no significant difference was detected in the deformation between the $\frac{1}{2}$ [541] band and the others.

The third calculation was performed with the configuration-dependent deformation parameter deduced by using the shell correction method with the Woods-Saxon potential and a monopole pairing residual interaction [28]. Unfortunately, the obtained ω_c in this case is 0.291 MeV (see Table IV), which is still too low. It should be pointed out that all the above calculations used the simple versions of the CSM with the deformation parameter determined by the ground state. Although the parameter was configuration dependent, its variation as a function of rotation was neglected.

There were two recent CSM calculations aimed at resolving this difficulty. First, using a deformed Woods-Saxon potential and the deformation parameter obtained from total Routhian surface (TRS), Yang *et al.* [32] obtained a similar (low) value of $\omega_c = 0.292$ MeV/ \hbar . The results for the odd Ta isotopes are listed in Table V.

TABLE IV. The deformation parameters used in various CSM calculations and the obtained crossing frequencies for the $\frac{1}{2}$ [541] band of ^{175}Ta and the yrast band of the even-even isotone. The deviation between theory and experiment in ω_c for the $\frac{1}{2}$ [541] band of ^{175}Ta is given in the last row.

| ε_2 | ε_4 | γ | $\hbar\omega_c(o-e)$ (MeV) | $\hbar\omega_c(e-e)$ (MeV) | $\Delta\hbar\omega_c$ (keV) |
|-------------------------|---------------------|-----------|-------------------------------|-------------------------------|--------------------------------|
| 0.250 [31] | 0.032 | 0^0 | 0.293 | 0.292 | 82 |
| 0.265 [28] | -0.016 | 0^0 | 0.291 | 0.290 | 84 |
| 0.290(β_2) [32] | -0.026(β_4) | -0.2 0 | 0.292 | 0.288 | 83 |
| 0.274 [33] | 0.031 | 1^0 | | | 40 |

Very recently, Chen [33] performed a CSM calculation which uses the Nilsson potential with configuration-dependent shape parameters ε_2 and γ obtained from the TRS calculation. The neutron gap parameter Δ_n was taken as $1.4\Delta_{oe}$ (the odd-even mass difference). The absolute value $\Delta\hbar\omega_c$ in this calculation is only about half of the observed value.

In Table IV, we have summarized the results of the above calculations. In the last row of this table, we see that there are large deviations between the theoretical and experimental crossing frequencies.

In early discussions along this line, the deficiencies of standard cranked shell model calculations including the monopole pairing force were discussed (see [34]). The inclusion of the quadrupole-pairing force resulted in an improved agreement with experiment for the description of the crossing frequency in rare-earth nuclei.

C. Summary of the CSM calculations

After examining various CSM calculations, one may conclude that this problem's resolution does not lie within the CSM framework. These CSM calculations with deformation parameters obtained from the TRS indicate that while the quadrupole deformation driving effect can have an effect, it is a minor one and cannot explain the delay of the AB band crossing frequency of the $\frac{1}{2}$ [541] proton orbital. Increasing the deformation ε_2 alone is insufficient to produce the absolute experimental crossing frequency. Such failures raise the question of whether the inadequacy of the mean field of the CSM, where the residual interactions can at best be partially and indirectly included [8,9], can address this problem.

TABLE V. Calculated neutron AB crossing frequencies of the $\frac{1}{2}$ [541] band for Ta isotopes and their even-even neighbors, and comparison of the theoretical and experimental delay in crossing frequency for the $\frac{1}{2}$ [541] band [32].

| Nucleus | $\hbar\omega_c(o-e)$ (MeV) | $\hbar\omega_c(e-e)$ (MeV) | $\Delta\hbar\omega_c(\text{Theor.})$ (keV) | $\Delta\hbar\omega_c(\text{Expt.})$ (keV) |
|-------------------|-------------------------------|-------------------------------|---|--|
| ^{167}Ta | 0.232 | 0.222 | 10 | 45 |
| ^{169}Ta | 0.242 | 0.233 | 9 | 40 |
| ^{171}Ta | 0.266 | 0.263 | 3 | 15 |
| ^{173}Ta | 0.280 | 0.274 | 6 | 65 |
| ^{175}Ta | 0.292 | 0.288 | 4 | 83 |

Hence, although the CSM has had much success in portraying the global features of a deformed heavy system, the inherent mean-field nature may render it difficult to quantitatively account for subtle features, such as those at or near the band crossing. In fact, without attempting to go beyond the mean field, it is not obvious how one could overcome this apparent failure [35].

IV. THE PROJECTED SHELL MODEL ANALYSIS

To go beyond the mean field, one needs to resort to a shell model approach. It is of course well known that a straightforward implementation of the shell model is impossible for heavy systems. The projected shell model [36] (PSM) is designed for this purpose. The PSM is in fact a shell model approach. Yet, unlike the conventional shell model, which begins with the spherically symmetric single-particle basis, the PSM begins with the deformed (Nilsson-type [37]) single-particle basis. Such a basis has the advantage of incorporating important nuclear correlations more readily, especially for a well-deformed system. Hence, in a manageable configuration space, one can treat the heavy systems in the shell model framework. Using the PSM, it has been demonstrated that one can quantitatively account for many high spin phenomena [38,39], and the results obtained can be interpreted in simple physical terms. While this shell model basis violates the rotational symmetry, it can be restored by the standard angular momentum projection technique [40]. The pairing correlation is included by successive BCS calculations for the Nilsson states. Thus, the shell model truncation is carried out within the quasiparticle states with the vacuum $|\phi\rangle$. Recently, based on the PSM, an alternative explanation of the anomalous crossing frequency in odd proton rare-earth nuclei has been suggested [10].

A. Theory

The ansatz for the angular-momentum-projected wave function is given by

$$|IM\rangle = \sum_{\kappa} f_{\kappa} \hat{P}_{MK}^I |\varphi_{\kappa}\rangle, \quad (4)$$

where κ labels the basis states. Acting on an intrinsic state $|\varphi_{\kappa}\rangle$, the operator \hat{P}_{MK}^I [40] generates states of good angular momentum, thus restoring the necessary rotational symmetry violated in the deformed mean field. The advantage of the present approach is that the crossing and mixing of bands at a given angular momentum are treated fully quantum mechanically. This turns out to be crucial to treat the present problem since the observed anomalies are consequences of the band crossings.

In the present work, we have assumed that the intrinsic states have axial symmetry. Thus, the basis states $|\varphi_{\kappa}\rangle$ must have K as a good quantum number. Since the nucleus in question has only a weak γ deformation, such a constraint will not prevent us from investigating the physics at hand. The basis states $|\varphi_{\kappa}\rangle$ are spanned by the set

$$\{\alpha_{p_l}^\dagger|\phi\rangle, \alpha_{n_i}^\dagger\alpha_{n_j}^\dagger\alpha_{p_l}^\dagger|\phi\rangle\},$$

$$\{|\phi\rangle, \alpha_{n_i}^\dagger\alpha_{n_j}^\dagger|\phi\rangle, \alpha_{p_k}^\dagger\alpha_{p_l}^\dagger|\phi\rangle, \alpha_{n_i}^\dagger\alpha_{n_j}^\dagger\alpha_{p_k}^\dagger\alpha_{p_l}^\dagger|\phi\rangle\}, \quad (5)$$

for odd proton and even-even nuclei, respectively. The quasiparticle vacuum is $|\phi\rangle$ and α_m (α_m^\dagger) is the quasiparticle (qp) annihilation (creation) operator for this vacuum; the index n_i (p_i) runs over selected neutron (proton) quasiparticle states and κ in Eq. (4) runs over the configuration of Eq. (5). The vacuum is obtained by diagonalizing a deformed Nilsson Hamiltonian [37] followed by a BCS calculation. In the calculation, we have used three major shells, i.e., $N=4, 5$, and 6 ($N=3, 4$, and 5) for neutrons (protons) as the configuration space. For the odd system, the BCS blocking effect associated with the last unpaired proton is taken into account by allowing all the odd number of protons to participate without blocking any individual level. The size of the basis states, which includes the most important configurations, is determined by using energy windows of 1.5 MeV, 2.5 MeV, 3 MeV, and 4 MeV for the 1qp, 2qp, 3qp, and 4qp states, respectively.

In this work we have used the Hamiltonian [36]

$$\hat{H} = \hat{H}_0 - \frac{1}{2} \chi \sum_{\mu} \hat{Q}_{\mu}^{\dagger} \hat{Q}_{\mu} - G_M \hat{P}^{\dagger} \hat{P} - G_Q \sum_{\mu} \hat{P}_{\mu}^{\dagger} \hat{P}_{\mu}, \quad (6)$$

where \hat{H}_0 is the spherical single-particle shell model Hamiltonian. The second term is the quadrupole-quadrupole interaction and the last two terms are the monopole and quadrupole pairing interactions, respectively. The interaction strengths are determined as follows: The quadrupole interaction strength χ is adjusted so that the known quadrupole deformation ε_2 from the Hartree-Fock-Bogoliubov self-consistent procedure [41] is obtained. It turns out that, for ^{175}Ta , $\varepsilon_2 = 0.260$. The monopole pairing strength G_M is adjusted to the known energy gap

$$G_M = \left[20.12 \mp 13.13 \frac{N-Z}{A} \right] A^{-1}, \quad (7)$$

where the minus (plus) sign is for neutrons (protons). The quadrupole pairing strength G_Q is assumed to be proportional to G_M and the proportional constant is fixed to be 0.24 in the present work. The effect of adjusting the quadrupole pairing will be discussed later.

The weights f_{κ} in Eq. (4) are determined by diagonalizing the Hamiltonian \hat{H} in the basis given by Eq. (5). This will lead to the eigenvalue equation (for a given spin I)

$$\sum_{\kappa'} (H_{\kappa\kappa'} - EN_{\kappa\kappa'}) f_{\kappa'} = 0, \quad (8)$$

with the Hamiltonian and norm overlaps given by

$$H_{\kappa\kappa'} = \langle \varphi_{\kappa} | \hat{H} \hat{P}_{\kappa\kappa'}^I | \varphi_{\kappa'} \rangle, \quad N_{\kappa\kappa'} = \langle \varphi_{\kappa} | \hat{P}_{\kappa\kappa'}^I | \varphi_{\kappa'} \rangle. \quad (9)$$

Projection of good angular momentum onto each intrinsic state generates the rotational band associated with this intrinsic configuration $|\varphi_{\kappa}\rangle$. For example, $\hat{P}_{MK}^I \alpha_{p_l}^\dagger |\phi\rangle$ will pro-

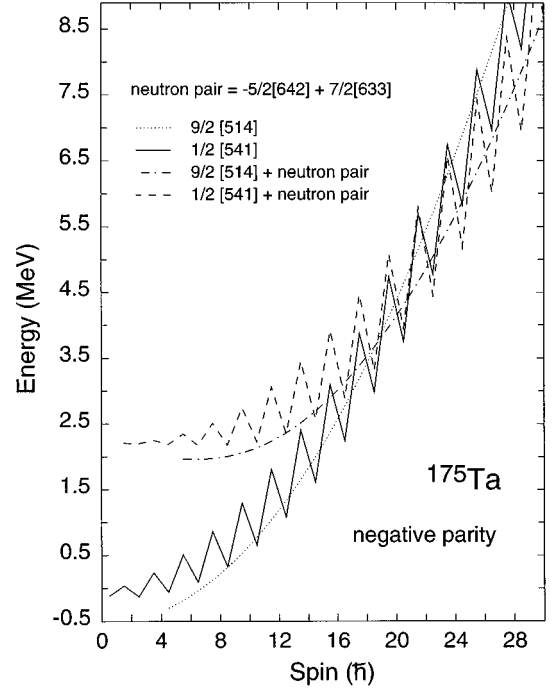


FIG. 7. Band diagram for negative parity bands in ^{175}Ta . Two-proton 1qp bands $\frac{9}{2}$ [514] and $\frac{1}{2}$ [541] and the corresponding 3qp bands are plotted.

duce a one-quasiproton band. The energies of each band are given by the diagonal elements of Eq. (9)

$$E_{\kappa}(I) = \frac{\langle \varphi_{\kappa} | \hat{H} \hat{P}_{\kappa\kappa}^I | \varphi_{\kappa} \rangle}{\langle \varphi_{\kappa} | \hat{P}_{\kappa\kappa}^I | \varphi_{\kappa} \rangle} = \frac{H_{\kappa\kappa}}{N_{\kappa\kappa}}. \quad (10)$$

A diagram in which $E_{\kappa}(I)$ of various bands are plotted against the spin I will be referred to [36] as a band diagram. It will reveal information to understand the character of the observed band crossings. The results obtained from diagonalizing the Hamiltonian of Eq. (6) can be compared with the experiments.

B. Comparison of the calculation with experiment

In Figs. 7 and 8, the band diagrams for negative and positive parity bands of ^{175}Ta are presented, respectively. Although the calculation produces more bands, for the present purpose, only the most interesting ones are plotted to illustrate the main features. The rotational frequency of each band, $\omega(I) = dE(I)/dI$, is naturally described by the slope of the curve and its inverted value by the moment of inertia.

In Fig. 7, one sees that for a given angular momentum, different configurations give rise to different slopes. As a function of increasing angular momentum, the $\frac{9}{2}$ [514] band shows the usual smooth behavior. From this figure, we see that it roughly crosses with the $\frac{1}{2}$ [541] band at spin $\frac{21}{2} \hbar$ and continues upward monotonously. At about spin $\frac{31}{2} \hbar$, it is a converging point of several bands and all will interact with each other. At this point, the empirical assignments of the levels cannot be clear-cut. From Fig. 7, we can predict that the $\frac{9}{2}$ [514] band will cross the 3qp band at spin $\frac{37}{2} \hbar$.

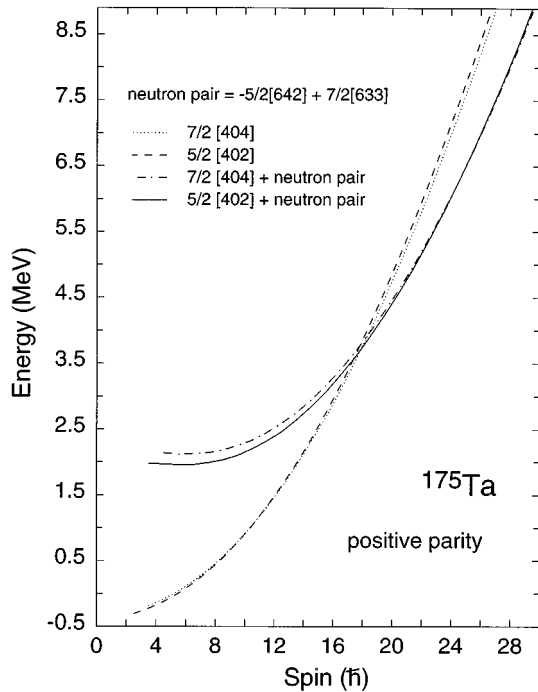


FIG. 8. Band diagram for positive parity bands in ^{175}Ta . Two-proton 1qp bands $\frac{5}{2} [402]$ and $\frac{7}{2} [404]$ and the corresponding 3qp bands are plotted.

For the $\frac{1}{2} [541]$ band, the zigzag behavior indicates that the energies have a strong signature splitting. In fact, one empirically observes the favored branch with signature $+\frac{1}{2}$. This one-quasiproton band crosses the 3qp band at spin $\frac{45}{2} \hbar$, thus producing the observed anomaly in the spectra. Beyond this point, the structure of the yrast band is mainly 3qp in nature. It should be pointed out that without any additional assumption, our calculation indicates that the $\frac{1}{2} [541]$ band crosses the 3qp band at a much later stage (spin $\frac{45}{2} \hbar$) than the $\frac{9}{2} [514]$ band (spin $\frac{37}{2} \hbar$). This means that from the PSM, band crossings are sensitively configuration dependent.

In Fig. 8 one sees the smooth behavior of the bands $\frac{5}{2} [402]$ and $\frac{7}{2} [404]$. This is quite similar to the $\frac{9}{2} [514]$ band. In fact, these two bands are found to be nearly degenerate. This was also observed in the ^{169}Ta calculation [42] and can thus be considered as a general feature for the Ta isotopes. Although their interaction causes a slight repulsion, the two bands nevertheless remain parallel and have nearly identical moments of inertia. It is predicted that the crossings will occur around spin $\frac{35}{2} \hbar$, which is clearly earlier than those of the negative parity bands (see Fig. 7).

In Fig. 9, the theoretical level scheme is presented. This was obtained by solving the eigenvalue equation (8) (band mixing). The seven lowest-lying positive and negative parity bands (to be compared with the measured levels in Fig. 1) are obtained by diagonalizing the matrix once (see Fig. 7 and Fig. 8 for their exact locations and the positions of band crossing). This calculation includes states up to spin $\frac{61}{2} \hbar$ for those with signature $+\frac{1}{2}$ and $\frac{59}{2} \hbar$ for those with $-\frac{1}{2}$. For higher spin states, we expect that 5qp states will be near the

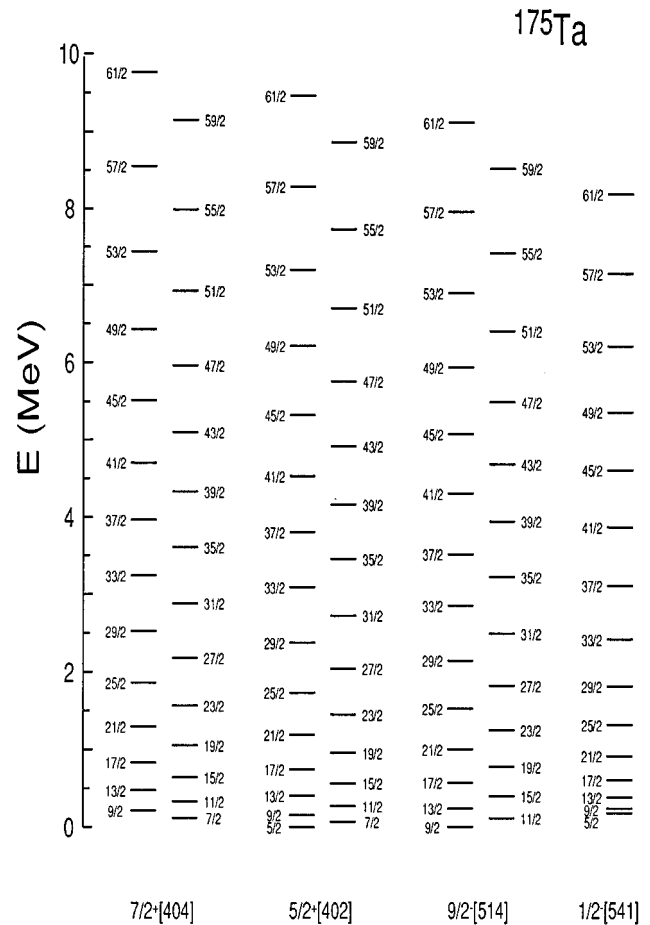


FIG. 9. Theoretical level scheme of ^{175}Ta , to be compared with Fig. 1.

yrast region and will be important. Since such configurations are absent here, it is reasonable that the predicted levels at very high spins are found to be too high in energy.

Experimentally, since the linking transitions are missing, the excitation energies of the bandheads are unknown. This calculation, on the other hand, suggests that the $I=\frac{5}{2}$ of the band $\frac{5}{2}^+ [402]$ is in fact the lowest and is regarded as the ground state ($E=0$) (see Fig. 9). The excitation energies of the other bandheads related to the ground state are 122 keV ($I=\frac{7}{2}$ in the $\frac{7}{2}^+ [404]$ band), 5 keV ($I=\frac{9}{2}$ in the $\frac{9}{2}^- [514]$ band), and 181 keV ($I=\frac{5}{2}$ in the $\frac{1}{2}^- [541]$ band). Although the $\frac{9}{2}^- [514]$ band has the lowest state at very low spins, due to the crossing with $\frac{1}{2}^- [541]$ band at spin $\frac{21}{2} \hbar$, the latter becomes the yrast band after that spin. The two positive parity bands $\frac{5}{2}^+ [402]$ and $\frac{7}{2}^+ [404]$, due to their interactions, are now shifted from each other in a parallel manner by roughly 100 keV at low spins. Still they roughly maintain identical transition energies.

C. Delay of the crossing and the quadrupole pairing interaction

In this section, we shall address the question of the delay in the band crossing of the proton $\frac{1}{2} [541]$ band. The results

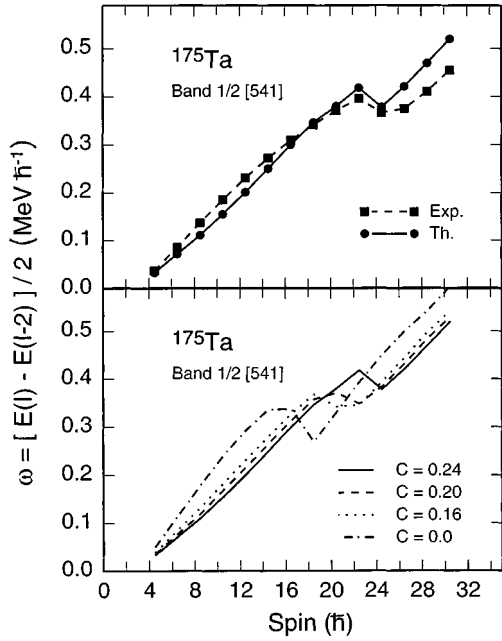


FIG. 10. Rotational frequency vs angular momentum plot for the proton $\frac{1}{2}$ [541] band in ^{175}Ta . (a) Top: comparison of the calculation with the present data. (b) Bottom: influence of the quadrupole pairing force on the crossing frequency.

of our calculations are shown by plotting the rotational frequency as a function of the angular momentum in Fig. 10. For Fig. 10(a), the PSM predictions agree well with the data. In particular, it reproduces the rotational alignment at spin $\frac{45}{2} \hbar$. It is interesting to notice the role played by the quadrupole pairing force in the Hamiltonian of Eq. (6), whose sensitive influence on the results is demonstrated in Fig. 10(b). Indeed, by increasing the C from 0.16 to 0.24, one obtains a significant delay of the alignment. If this force is absent from the Hamiltonian (i.e., $C = 0$), the alignment can occur as early as spin $\frac{33}{2} \hbar$. The physical reason behind the delay is as follows: If a zero angular momentum pair is broken in the absence of quadrupole pairing, then there is no additional force to resist the alignment process beyond that point [43,10]. In other words, the quadrupole pairing interaction prevents the alignment from occurring too early.

As was mentioned at the beginning, the delay of the crossing frequency is measured by comparing an odd- Z nucleus with its even-even neighbors. Hence a unified treatment demands us to examine the even-even neighboring nuclei with the same theory as well. In Fig. 11, we present our results for ^{174}Hf and ^{176}W . By varying the quadrupole pairing strength, one observes the effect of shifting the crossing points. However, because of stronger band interactions, the influence of varied quadrupole pairing strength cannot be seen as clearly as in the ^{175}Ta case [see Fig. 10(b)]. Further inspection of the dynamical moment of inertia ($\mathcal{J}^{(2)}$) indicates that for ^{176}W , one can reproduce the peak of $\mathcal{J}^{(2)}$ at $I = 18$ when a quadrupole pairing strength $C = 0.20 - 0.24$ is used, while for ^{174}Hf , a smaller $C = 0.16$ is required to reproduce the peak of $\mathcal{J}^{(2)}$ at $I = 16$. This implies that the force can be dependent on the mass number (for further discussion, see the last paragraph of this subsection). Furthermore,

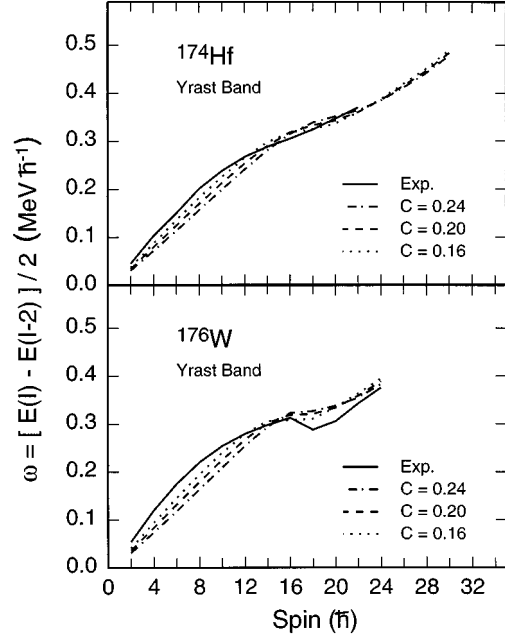


FIG. 11. Rotational frequency vs angular momentum plot for the yrast band of the two isotones ^{174}Hf and ^{176}W . Data are taken from ^{174}Hf [29] and ^{176}W [30]. The influence of the quadrupole pairing force on the crossing frequency is shown.

we noticed that the effect is less pronounced at very low spins than higher spins, as seen in Fig. 10(b).

As summarized in Sec. III, one cannot account for the absolute value of the observed crossing frequency by merely changing deformation ε_2 alone in the CSM. The question of what is the effect of the deformed field to the shift of the crossing cannot be answered directly within the present model because the deformed single-particle scheme serves in the PSM only as a basis from which the many-body wave functions are constructed. Since the physics should be basis independent, the physical consequence must emerge from any suitably chosen basis provided no additional effects (e.g., caused by basis truncation) are introduced. In Ref. [10], we stressed that including both the quadrupole pairing interaction and the shell model configuration mixing is important for the PSM to reproduce the observed delay of the crossing frequency. It would be interesting to see how the CSM results can be improved by including this force. However, we would like to point out that in the PSM, angular momentum projection generates states in the laboratory system and ensures the states to be mixed (1) by two-body residual interactions and (2) at a given angular momentum (not a given rotational frequency). We believe that these two ingredients are important for a more complete description of the phenomenon at hand. Clearly, both of these ingredients are missing in the CSM.

The quadrupole pairing has not been studied as much as other effective interactions. Therefore, it will be interesting to see if one could gain additional information and insight about this interaction from the study of high spin spectroscopy. The quadrupole pairing strength is an adjustable parameter according to the PSM. The average ratio of the strengths of quadrupole and monopole pairing used in the

PSM is 0.2 [36], a value which is consistent with that introduced by Refs. [44,45].

At this stage, what we have done is to confirm the significant contribution from the quadrupole pairing interaction to the anomalous crossing frequency. It is important to note that the PSM is able to account for the trend of the variation of the crossing frequency as a function of mass number. In fact, preliminary results obtained by the PSM satisfactorily reproduce the crossing frequencies for all the odd proton nuclei in the rare-earth region by adjusting the quadrupole-pairing interaction (with the ratio of the strengths of quadrupole and monopole pairing varying from 0.16 to 0.24) only [46]. In particular, the V shape of the observed shift in the Ta isotope chain (as discussed in Sec. III) is successfully reproduced. Adjustment of this parameter around the average value for different nuclei (e.g., along an isotope chain) may indicate the orbital-dependent nature of this force. Work towards understanding this problem is in progress.

V. SUMMARY

In this paper, the high spin states in ^{175}Ta were studied. A new experimental level scheme is presented. The data show

that for this nucleus, the shift in crossing frequency for the $\frac{1}{2}$ [541] proton band is the largest one observed to date. In order to understand this shift, we have performed several versions of CSM calculations and found that none can quantitatively reproduce this feature. Thus, from these CSM studies it is difficult to ascertain which mechanism within the CSM framework, if any, is the leading cause for this observation. On the other hand, the PSM is able to reproduce the measurement satisfactorily. The essential difference between the PSM and the CSM is that the former is a fully quantum mechanical theory and treats the band crossings properly. One of the effective interactions, the quadrupole pairing force, is found to be responsible for the observed delay. It is therefore suggestive that a systematic investigation of the crossing frequency may open a new empirical window to study this subtle effective interaction.

ACKNOWLEDGMENTS

Financial support is acknowledged from the China National Nuclear Industry Corporation, National Science Foundation of China, and U. S. National Science Foundation.

-
- [1] C. Foin, S. Andre, and D. Barneoud, *Phys. Rev. Lett.* **35**, 1697 (1975).
- [2] A. Neskakis, R.M. Lieder, M. Müller-Veggian, H. Beuscher, W.F. Davidson, and C. Mayer-Böricke, *Nucl. Phys.* **A261**, 189 (1976).
- [3] A. Faessler, M. Ploszajczak, and K.R. Sandhya, *Nucl. Phys.* **A301**, 382 (1978).
- [4] S. Frauendorf, *Phys. Scr.* **24**, 349 (1981).
- [5] C.H. Yu, G.B. Hagemann, J.M. Espino, K. Furuno, J.D. Garrett, R. Chapman, D. Clarke, F. Khazaie, J.C. Lisle, J.N. Mo, M. Bergström, L. Carlen, P. Ekström, J. Lyttkens, and H. Ryde, *Nucl. Phys.* **A511**, 157 (1990).
- [6] H. Jensen, G.B. Hagemann, P.O. Tjom, A. Atac, M. Bergström, A. Bracco, A. Brockstedt, H. Carlsson, P. Ekström, J.M. Espino, S. Frauendorf, B. Herskind, E. Ingebretsen, J. Jongman, S. Leoni, R.M. Lieder, T. Lönnroth, A. Maj, B. Million, A. Nordlund, J. Nyberg, M. Piiparinen, H. Ryde, M. Sugawara, and A. Virtanen, *Z. Phys. A* **340**, 351 (1991).
- [7] L.L. Riedinger, J. Avakian, H.-Q. Jin, W.F. Mueller, and C.-H. Yu, *Prog. Part. Nucl. Phys.* **28**, 75 (1992).
- [8] R. Wyss, presented at the workshop symposium on Reflection and Directions in Low Energy Heavy-Ion Physics, Joint Institute for Heavy Ion Physics, Oak Ridge, Tennessee, 1991 (unpublished).
- [9] W. Satula, R. Wyss, and F. Dönau, *Nucl. Phys.* **A565**, 573 (1993).
- [10] Y. Sun, S. Wen, and D.H. Feng, *Phys. Rev. Lett.* **72**, 3483 (1994).
- [11] C.S. Wu, *Phys. Rev. C* **51**, 1819 (1995).
- [12] K. Theine, C.X. Yang, A.P. Byrue, H. Huble, R. Chapman, D. Clarke, F. Khazaie, J. C. Lisle, J.N. Mo, J.D. Garrett, and H. Ryde, *Nucl. Phys.* **A536**, 418 (1993).
- [13] S.G. Li, S. Wen, G.J. Yuan, G.S. Li, P.F. Hua, L.K. Zhang, Z.K. Yu, P.S. Yu, P.K. Weng, C.X. Yang, R. Chapman, D. Clarke, F. Khazaie, J.C. Lisle, J.N. Mo, J.D. Garrett, G.B. Hagemann, B. Herskind, and H. Ryde, *Nucl. Phys.* **A555**, 435 (1993).
- [14] J.C. Bacelar, R. Chapman, J.R. Leslie, J.C. Lisle, J. N. Mo, E. Paul, A. Simcock, J.C. Willmott, J.D. Garrett, G.B. Hagemann, B. Herskind, A. Holm, and P. M. Walker, *Nucl. Phys.* **A442**, 547 (1985).
- [15] H. Carlsson, R.A. Bark, L.P. Ekström, A. Nordlund, H. Ryde, G.B. Hagemann, S.J. Freemann, H.J. Jensen, T. Lönnroth, M.J. Piiparinen, H. Schnack-Petersen, F. Ingebretsen, and P.O. Tjom, *Nucl. Phys.* **A592**, 89 (1995).
- [16] D.E. Archer, M.A. Riley, T.B. Brown, J. Döring, D.J. Hartley, G.D. Johns, T.D. Johnson, R.A. Kaye, J. Pfohl, S.L. Tabor, J. Simpson, and Y. Sun, *Phys. Rev. C* **52**, 1326 (1995).
- [17] J. Gascon, C.-H. Yu, G.B. Hagemann, M.C. Carpenter, J.M. Espino, Y. Iwata, T. Komatsubara, J. Nyberg, S. Ogaza, G. Sletten, P.O. Tjom, D.C. Radford, J. Simpson, A. Alderson, M.A. Bentley, P. Fallon, P.D. Forsyth, J.W. Roberts, and J.F. Sharpey-Schafer, *Nucl. Phys.* **A513**, 344 (1990).
- [18] S. Jonson, J. Lyttkens, L. Carlen, N. Roy, H. Ryde, and W. Walus, *Nucl. Phys.* **A422**, 397 (1984).
- [19] R.A. Berk, G.D. Dracoulis, A.E. Stuchbery, A.P. Byrne, A.M. Baxter, F. Riess, P.K. Weng, S. Jonson, J. Lyttkens, L. Carlen, N. Roy, H. Ryde, and W. Walus, *Nucl. Phys.* **A501**, 157 (1989).
- [20] C.X. Yang, S.G. Li, S. Wen, G.S. Li, G.J. Yuan, P.S. Yu, and P.K. Weng, in *Proceedings of International Symposium on Heavy Ion Physics and its Application*, Lanzhou, China, 1990 p. 434 (unpublished).
- [21] P. Möller and I.R. Nix, *At. Data Nucl. Data Tables* **26**, 165 (1981).
- [22] C. Foin, Th. Lindblad, B. Skanberg, and H. Ryde, *Nucl. Phys.* **A195**, 465 (1972).
- [23] S. Wen, H. Zheng, S.G. Li, G.S. Li, G.J. Yuan, P.F. Hua, P.K.

- Weng, L.K. Zhang, P.S. Yu, C.X. Yang, H.B. Sun, Y.B. Liu, and Y.Z. Liu, *Z. Phys. A* **339**, 417 (1991).
- [24] R. Bengtsson and S. Frauendorf, *Nucl. Phys.* **A327**, 139 (1979).
- [25] R. Bengtsson and J.D. Garrett, *Collective Phenomena in Atomic Nuclei*, International Review of Nuclear Physics, Vol. 2 (World Scientific, Singapore, 1984), p. 194.
- [26] A.F. Dónau, *Nucl. Phys.* **A471**, 469 (1987).
- [27] A.J. Larabee, L.H. Courtney, S. Frauendorf, L.L. Riedinger, J.C. Weddington, M.P. Fewell, N.R. Johnson, I.Y. Lee, and F.K. McGouDan, *Phys. Rev. C* **29**, 1934 (1984).
- [28] W. Nazarewicz, M.A. Riley, and J.D. Garrett, *Nucl. Phys.* **A512**, 61 (1990).
- [29] P.M. Walder, P.V. Arve, J. Simpson, G.B. Hagemann, J. Pedersen, G. Sletten, M.A. Riley, D. Howe, B.M. Nyakv, J.R. Sharpey-Schafer, J.C. Lisle, and E. Paul, *Phys. Lett.* **168B**, 326 (1986).
- [30] I.Y. Lee, C. Baktash, and J.X. Saladin, *Phys. Rev. C* **29**, 837 (1984).
- [31] A.H. Wapstran and G. Audi, *Nucl. Phys. A* **432**, 1 (1985).
- [32] C.X. Yang, S. Wen, S.G. Li, G.J. Yuan, P.K. Weng, G.S. Li, and J.N. Mo, *J. Chin. Nucl. Phys.* (submitted).
- [33] Y.S. Chen (private communication); J. Chin, *Nucl. Phys.* (submitted).
- [34] M. Diebel, *Nucl. Phys.* **A419**, 221 (1984).
- [35] Y. Sun and D.H. Feng, *Phys. Rep.* **264**, 375 (1996).
- [36] K. Hara and Y. Sun, *Int. J. Mod. Phys. E* **4**, 637 (1995).
- [37] C.G. Andersson, G. Hellström, G. Leander, I. Ragnarsson, S. Åberg, J. Krumlinde, S.G. Nilsson, and Z. Szymański, *Nucl. Phys.* **A309**, 141 (1978).
- [38] H. Hara and Y. Sun, *Nucl. Phys.* **A529**, 445 (1991); **A531**, 221 (1991); **A537**, 77 (1992).
- [39] Y. Sun and J.L. Egidio, *Nucl. Phys.* **A580**, 1 (1994); *Phys. Rev. C* **50**, 1893 (1994).
- [40] P. Ring and P. Schuck, *The Nuclear Many Body Problem* (Springer-Verlag, Berlin, 1980).
- [41] I.L. Lamm, *Nucl. Phys.* **A125**, 504 (1969).
- [42] Y. Sun, D.H. Feng, and S. Wen, *Phys. Rev. C* **50**, 2351 (1994).
- [43] M. Wakai and A. Faessler, *Nucl. Phys.* **A295**, 86 (1978).
- [44] B.A. Broglia, D.R. Bes, and B.S. Nilsson, *Phys. Lett.* **50B**, 213 (1974).
- [45] H. Sakamoto and T. Kishimoto, *Phys. Lett. B* **245**, 321 (1990).
- [46] Y. Sun *et al.* (unpublished).